Co-Precipitation of Radium with Barium and Strontium Sulfate and Its Impact on the Fate of Radium during Treatment of Produced Water from Unconventional Gas Extraction

ARTICLE *in* ENVIRONMENTAL SCIENCE & TECHNOLOGY · MARCH 2014

Impact Factor: 5.33 · DOI: 10.1021/es405168b · Source: PubMed

4 AUTHORS, INCLUDING:

Tieyuan Zhang
University of Pittsburgh
4 PUBLICATIONS **21** CITATIONS
SEE PROFILE

Kelvin B Gregory
Carnegie Mellon University
48 PUBLICATIONS **1,693** CITATIONS
SEE PROFILE

Radisav D Vidic
University of Pittsburgh
150 PUBLICATIONS **2,917** CITATIONS
SEE PROFILE

Environmental Science & Technology

Article

pubs.acs.org/est

Co-precipitation of Radium with Barium and Strontium Sulfate and Its Impact on the Fate of Radium during Treatment of Produced Water from Unconventional Gas Extraction

Tieyuan Zhang,[†,‡] Kelvin Gregory,[§,‡] Richard W. Hammack,[‡] and Radisav D. Vidic*[,†,‡]

[†]Department of Civil and Environmental Engineering, University of Pittsburgh, Pittsburgh, Pennsylvania 15261, United States

[‡]National Energy Technology Laboratory (NETL), Pittsburgh, Pennsylvania 15236, United States

[§]Department of Civil and Environmental Engineering, Carnegie Mellon University, Pittsburgh, Pennsylvania 15213, United States

Supporting Information

ABSTRACT: Radium occurs in flowback and produced waters from hydraulic fracturing for unconventional gas extraction along with high concentrations of barium and strontium and elevated salinity. Radium is often removed from this wastewater by co-precipitation with barium or other alkaline earth metals. The distribution equation for Ra in the precipitate is derived from the equilibrium of the lattice replacement reaction (inclusion) between the Ra^{2+} ion and the carrier ions (e.g., Ba^{2+} and Sr^{2+}) in aqueous and solid phases and is often applied to describe the fate of radium in these systems. Although the theoretical distribution coefficient for Ra−$SrSO_4$ (K_d = 237) is much larger than that for Ra−$BaSO_4$ (K_d = 1.54), previous studies have focused on Ra−$BaSO_4$ equilibrium. This study evaluates the equilibria and kinetics of co-precipitation reactions in Ra−Ba−SO_4 and Ra−Sr−SO_4 binary systems and the Ra−Ba−Sr−SO_4 ternary system under varying ionic strength (IS) conditions that are representative of brines generated during unconventional gas extraction. Results show that radium removal generally follows the theoretical distribution law in binary systems and is enhanced in the Ra−Ba−SO_4 system and restrained in the Ra−Sr−SO_4 system by high IS. However, the experimental distribution coefficient (K_d') varies widely and cannot be accurately described by the distribution equation, which depends on IS, kinetics of carrier precipitation and does not account for radium removal by adsorption. Radium removal in the ternary system is controlled by the co-precipitation of Ra−Ba−SO_4, which is attributed to the rapid $BaSO_4$ nucleation rate and closer ionic radii of Ra^{2+} with Ba^{2+} than with Sr^{2+}. Carrier (i.e., barite) recycling during water treatment was shown to be effective in enhancing radium removal even after co-precipitation was completed. Calculations based on experimental results show that Ra levels in the precipitate generated in centralized waste treatment facilities far exceed regulatory limits for disposal in municipal sanitary landfills and require careful monitoring of allowed source term loading (ASTL) for technically enhanced naturally occurring materials (TENORM) in these landfills. Several alternatives for sustainable management of TENORM are discussed.

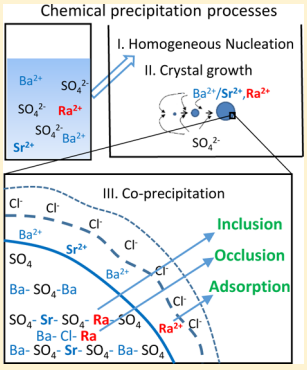

INTRODUCTION

Radium-226/228 is formed by natural decay of uranium-238 and thorium-232 and occurs in natural gas brines brought to the surface following hydraulic fracturing.[1] Because radium is relatively soluble over a wide range of pH and redox conditions, it is the dominant naturally occurring radioactive material (NORM) and an important proxy for radioactivity of waste streams produced during unconventional gas extraction.[2,3] Radium is a member of alkaline-earth group metals and has properties similar to calcium, strontium, and barium. Oral radium uptake can lead to substitution of calcium in bones and ultimately long-term health risks. Radium-226 activity in Marcellus-Shale-produced water ranges from hundreds to thousands picocuries per liter (pCi/L), with a median of 5350 pCi/L.[1] The total radium limit for drinking water and industrial effluents is 5 and 60 pCi/L, respectively.[4]

Radium activity in flowback water from the Marcellus Shale play shows positive correlation with total dissolved solids (TDS) and barium content, despite the differences in reservoir lithologies.[1,5] This finding is consistent with the fact that the radium/barium ratio is often constant in unconfined aquifers, implying that the radium co-precipitation into barite controls the activity of radium.[6] The high TDS (680−345 000 mg/L)[7] in produced water from Marcellus Shale gas wells is one of the main considerations when choosing a proper radium treatment technology. While there are several treatment options for radium removal, none is as cost-effective in high TDS brines as sulfate precipitation.[8] Despite a very low solubility product for $RaSO_4$ ($K_{sp,RaSO_4} = 10^{-10.38}$),[9] it is not likely to observe pure $RaSO_4$ precipitate because of very low radium concentrations in the produced water. However, radium may co-precipitate with other carrier metals.

Received: November 21, 2013
Revised: March 25, 2014
Accepted: March 26, 2014
Published: March 26, 2014

   dx.doi.org/10.1021/es405168b | Environ. Sci. Technol. 2014, 48, 4596−4603

A distribution equation has been used to describe the co-precipitation of a soluble tracer with a carrier ion. Sulfate-based co-precipitation of radium in a binary system with barium has been examined previously[6,9−12] and is described by the following distribution equation:

$$\frac{RaSO_4}{MSO_4} = K_d \frac{Ra^{2+}}{M^{2+}}$$

where K_d is the concentration-based effective distribution coefficient, MSO_4 and $RaSO_4$ are relative fractions (or "concentrations") of carrier and radium in solid precipitate, and M^{2+} and Ra^{2+} are equilibrium concentrations in solution. Derivation of the theoretical distribution coefficient with associated thermodynamic parameters is summarized in the Supporting Information and Tables SI-1 and SI-2 of the Supporting Information. Theoretical distribution coefficients of Ra in $BaSO_4$ and $SrSO_4$ in dilute solution are 1.54 and 237, respectively. An increase in the ionic strength (IS) of solution would lead to a decrease in the activity coefficients for Ra^{2+}, Ba^{2+}, and Sr^{2+}, as shown on Figure SI-1 of the Supporting Information. Changes in the activity coefficient ratio of tracer and carrier ion, which is critical when calculating the distribution coefficient in binary systems (see eq 9 of the Supporting Information), are much more pronounced in the case of Sr^{2+} than Ba^{2+} (see Figure SI-1 of the Supporting Information). Consequently, the theoretical distribution coefficient for Ra−Sr−SO_4 exhibits more than 50% decline when the IS increased to 3 M, while the decrease in the case of Ra−Ba−SO_4 was less than 10% (Figure 1). On the basis of this

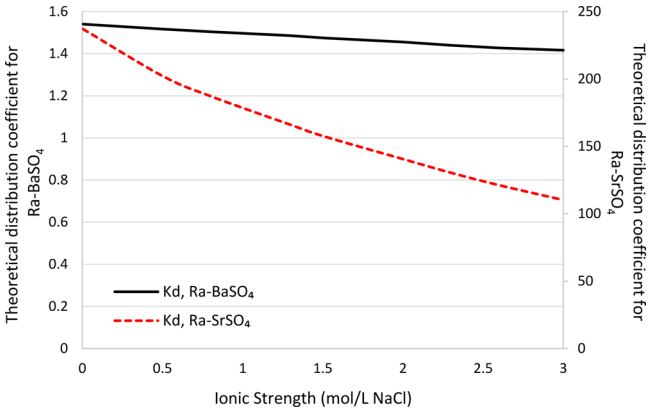

Figure 1. Theoretical distribution coefficient ($K_{d,Ra-MSO_4}$) for radium in $BaSO_4$ and $SrSO_4$ as a function of the IS based on eq 9 of the Supporting Information.

analysis, it can be expected that an increase in the IS of solution would have a much greater impact on the removal of Ra^{2+} by co-precipitation with $SrSO_4$ than with $BaSO_4$.

Even though the distribution equation has been used to explain the co-precipitation reactions, it has several limitations. First, the presence of electrolytes in solution changes the surface properties (i.e., particle size/morphology, etch pits, etc.) of the carrier[13] and affects radium removal. Second, the distribution equation assumes that the ions in solution are in equilibrium with the ions throughout the entire solid phase.[14] However, the degree of Ra incorporated into the crystal would be uneven throughout the co-precipitation process if the crystal growth rate is faster than the rate of lattice replacement because the lattice replacement has not reached equilibrium during nucleation and crystal growth. A previous study[15] showed that reduction in the barite precipitation rate significantly increased Ra removal by co-precipitation.

In addition, co-precipitation is a broad term to illustrate the phenomenon where a soluble substance is included in a carrier precipitate, which actually involves three distinct mechanisms: inclusion, occlusion, and adsorption (Figure 2).[15] Inclusion or

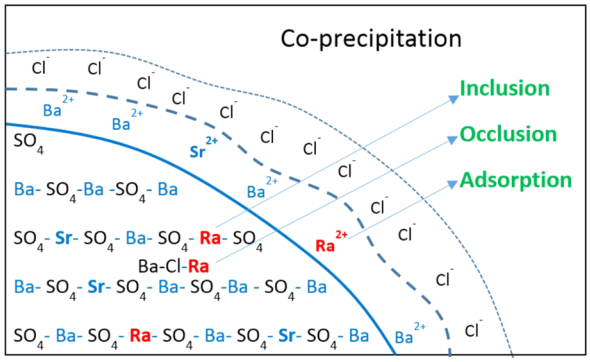

Figure 2. Three mechanisms (inclusion, occlusion, and adsorption) of radium co-precipitation in binary solution with Ba−SO_4

lattice replacement reaction occurs when a tracer (i.e., Ra^{2+}) occupies a lattice site in the carrier mineral (e.g., barite and celestite), resulting in a crystallographic defect with the tracer in place of the main cation. Occlusion refers to the phenomenon where a tracer is physically trapped inside the crystal during crystal growth, which can be explained by the entrapment of solution or adsorption of tracer during the crystal growth.[15−18] However, occlusion is not likely to play a major role in Ra removal during barite precipitation because of the low moisture content of barite crystal (<3.5%)[16] and because Ra is present in solution at very low levels. Adsorption occurs when the tracer is weakly bound at the surface of the precipitate.[15] As described in the Supporting Information, the distribution equation reflects only the inclusion (lattice replacement) mechanism while neglecting contributions to tracer uptake by adsorption and occlusion. Even though occlusion is a minor mechanism for Ra removal, neglecting adsorption and occlusion during tracer uptake and kinetic effects would inevitably lead to uncertainty in theoretical predictions.[6]

This study focuses on understanding the fundamental mechanisms of Ra co-precipitation in Ba/Sr−SO_4 binary and ternary systems at high saturation levels and different ISs. The mechanisms of inclusion and adsorption for Ra incorporation in the precipitate were distinguished by carefully controlling test conditions, so that the experimentally determined distribution of key species in both Ra−Ba−SO_4 and Ra−Sr−SO_4 co-precipitation experiments can be compared to theoretical predictions and Ra leaching from solids generated during co-precipitation and post-precipitation studies. The impact of precipitation kinetics, activity coefficient ratios, and volumetric mismatch between substituting end-members were analyzed as key factors influencing the fate of radium during co-precipitation with barite and celestite. Additionally, uptake of radium by barite and celestite post-precipitation was compared to the co-precipitation process to understand the relative impact of inclusion, occlusion, and adsorption on the overall radium removal by sulfate precipitation. This study further elucidates fundamental mechanisms influencing the fate of radium during chemical precipitation of divalent cations from

dx.doi.org/10.1021/es405168b | Environ. Sci. Technol. 2014, 48, 4596−4603

Table 1. Experimental Conditions for Ra Removal in Binary and Ternary Systems[32] [a]

	initial concentration				ion activity				SI	
system	NaCl (mol/L)	Ba (mmol/L)	Sr (mmol/L)	SO_4 (mmol/L)	IS (mol)	Ba (mmol/L)	Sr (mmol/L)	SO_4 (mmol/L)	SI_{BaSO_4}	SI_{SrSO_4}
Ba−Ra−SO_4 binary	0	5	0	0.5	0.0165	3.155		0.173	3.71	
		5	0	1.25	0.01875	2.943		0.483	4.09	
		5	0	5	0.03	2.146		1.9	4.58	
	3	5	0	0.5	3.0165	1.276		0.02	2.22	
		5	0	1.25	3.01875	1.277		0.349	2.62	
		5	0	5	3.03	1.285		0.139	3.22	
Sr−Ra−SO_4 binary	0	0	5	1.25	0.01875		3.01	0.537		0.85
		0	5	5	0.03		2.323	2.143		1.33
		0	5	10	0.045		1.773	4.164		1.51
	3	0	5	5	3.03		2.246	0.137		0.13
		0	5	10	3.045		2.234	0.273		0.42
		0	5	20	3.075		2.21	0.542		0.72
		0	5	50	3.165		2.142	1.324		1.09
Ba−Sr−Ra−SO_4 ternary	0	5	5	1.25	0.03375	2.674	2.767	0.339	3.92	0.6
		5	5	5	0.045	2.166	2.417	1.453	4.47	1.18
		5	5	10	0.06	1.702	2.016	3.064	4.69	1.43
	3	5	5	1.25	3.03375	1.279	2.255	0.035	2.62	−0.47
		5	5	5	3.045	1.286	2.246	1.382	3.22	0.13
		5	5	10	3.06	1.296	2.233	0.275	3.52	0.43

[a] SI = log(IAP/K_{SP}), where IAP is the ion activity product and K_{SP} is the solubility product. IS was adjusted with NaCl. Activity coefficients were calculated using Pitzer equation.

produced water (i.e., sulfate precipitation) and associated implications for its reuse for hydraulic fracturing following treatment.

MATERIALS AND METHODS

Radium-226 source was obtained from Pennsylvania State University and analyzed using a gamma spectrometer[23] with a high-purity germanium detector (Canberra BE 202). Barium chloride dihydrate (99.0% minimum, Mallinckrodt Chemicals), strontium chloride hexahydrate (99.0%, Acros Organics), sodium chloride (99.8%, Fisher Scientific), anhydrous sodium sulfate (100%, granular powder, J.T. Baker), trace-metal-grade nitric acid (65−70%, Fisher), and trace-metal-grade hydrochloric acid (37.3%, Fisher) were American Chemical Society (ACS)-grade. Commercial standards (Ricca Chemicals and Fisher) were used to calibrate atomic absorption spectrophotometer, and Ultima Gold high-flash-point liquid scintillation counting (LSC) cocktail (PerkinElmer) was used for the liquid scintillation counter. All reagents were tested and found to be free of radium.

The concentration of dissolved Ba and Sr was measured by atomic absorption spectrometry (PerkinElmer model 1000 AAS) with a nitrous oxide−acetylene flame. The filtrate was diluted in a 2% nitric acid and 0.15% KCl solution prior to analysis to limit interferences during metal analysis. Dilution ratios were chosen on the basis of the linear range of this instrument.

Radium-226 activity was analyzed using Packard 2100 LSC through the direct measurement of radium-226.[19] A total of 4 mL of the liquid sample was mixed with 14 mL of Ultima Gold universal LSC cocktail and counted by LSC for 60 min in the specific energy range (170−230 keV) to reject any contribution that is not produced by radium-226. The sample with high IS was corrected by the quench factor, and the ingrowth of radioactivity was compensated by the ingrowth factor.[19,20] Samples were occasionally calibrated by a gamma spectrometer[21] to ensure accuracy of radium-226 detection, especially at different salinities. Results showed that LSC analysis deviated from gamma spectrometry by less than 7.4%. Activity in both liquid and solid was measured for selected samples to validate the mass balance for radium-226.

Co-precipitation experiments were performed in 50 mL high-density polyethylene (HDPE) tubes. IS was adjusted to 1, 2, or 3 mol/L with concentrated NaCl solution. Radium-226 stock solution was diluted to a target level of 10 000 pCi/L, and the initial Ba^{2+} and Sr^{2+} concentrations were always 5 mmol/L. Different doses of sodium sulfate were added to adjust barium and strontium removal, and pH was not controlled in these experiments. HDPE tubes were placed on a horizontal shaker to promote mixing. Aqueous samples were taken after 24 h of reaction and filtered through 0.45 μm mixed cellulose ester membranes (MF-Millipore, HAWP) prior to analysis for radium-226, barium, and strontium. Because of the relatively slow kinetics of $SrSO_4$ formation,[13] Ra−Sr−SO_4 solutions were sampled after 5, 24, and 48 h.

Radium removal by barite/celestite post-precipitation was studied by adding a specific amount of preformed solids (barite and/or celestite) into 10 000 pCi/L radium-226 solution. Barite and celestite were prepared from the solution composition that is identical to that used in co-precipitation experiments to ensure identical particle morphology and size. After 24 h of moderate shaking, aqueous samples were removed and filtered through a 0.45 μm membrane prior to radium-226 analysis.

Experiments were performed to examine the equilibrium and kinetics of Ra−Ba−SO_4 and Ra−Sr−SO_4 formation alone and in combination using the initial conditions listed in Table 1. The binary and ternary systems were studied at high IS to simulate radium removal from brines generated by unconventional gas extraction. The distribution coefficient was calculated for each system and compared to theoretical values. Both kinetics and equilibrium studies were conducted to provide a fundamental understanding of the fate of radium during

chemical precipitation, employed to remove divalent cations from natural gas brines (i.e., sulfate precipitation) and facilitate its reuse for hydraulic fracturing.

RESULTS AND DISCUSSION

Impact of IS on Ra Removal by Co-precipitation in Binary Systems. The radium removal and experimental distribution coefficient (K_d') for Ra−Ba−SO_4 co-precipitation at different ISs is shown in Figure 3a. Radium co-precipitation

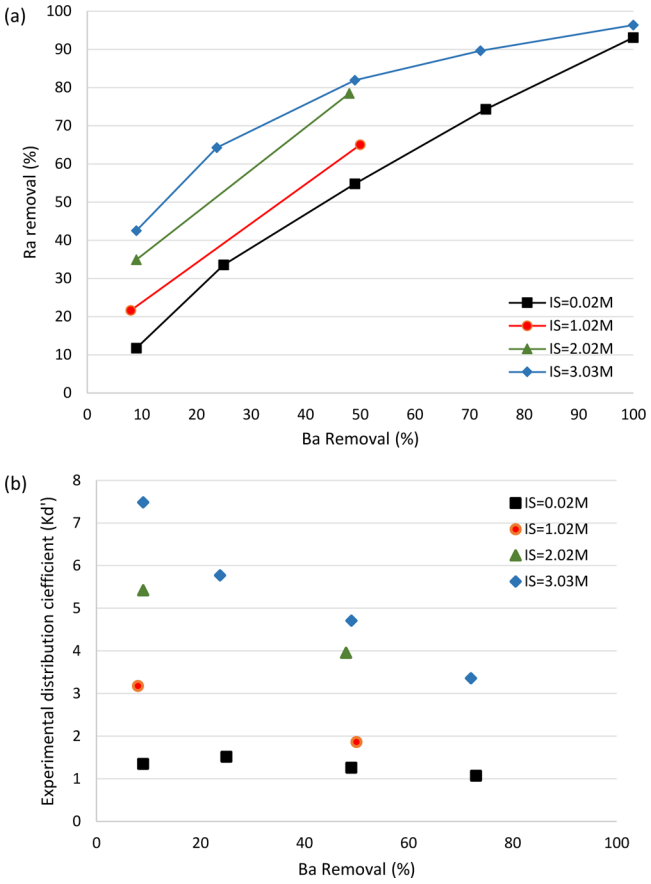

Figure 3. Radium co-precipitation with $BaSO_4$ as a function of barium removal at different ISs adjusted with NaCl: (a) radium removal and (b) experimental distribution coefficient, at pH 7 and 5 mM $Ba^{2+}_{initial}$. Ba removal was adjusted with sulfate addition.

in dilute solutions (i.e., IS of about 0.02 was due to the addition of $BaCl_2$ and Na_2SO_4 only) was proportional to barium removal, which can be described by the distribution law. The decrease of K_d' with the increase in Ba removal is expected because the inclusion of Ra into $BaSO_4$ during the initial stages of $BaSO_4$ precipitation decreases the Ra concentration in solution, resulting in a much lower Ra concentration to co-precipitate with subsequent $BaSO_4$. The experimental distribution coefficient (K_d' = 1.07−1.54) was always below the theoretical value (K_d = 1.54) in dilute solutions, which can be attributed to the fast barite crystal growth at high supersaturation levels used in these experiments [saturation index (SI) = 3.7−4.6]. Under these conditions, barite precipitation was completed within just 10 min, which adversely impacts radium removal because inclusion and occlusion processes only occur during nucleation and crystal growth of barite. Rosenberg et al.[22] reported that experimental K_d' can be as high as 3 when precipitation kinetics is controlled by continuously adjusting the concentration of reactants in the solution.

The dependence of the distribution coefficient upon IS (Figure 1) suggests only a slight decrease in K_d for Ra−Ba−SO_4 with an increase in IS. However, experimental results show that radium co-precipitation was enhanced in the presence of electrolytes, with experimental K_d' increasing to 3.17 at IS of 1.02 M and 7.49 at IS of 3.03 M for barium removal of 10% (Figure 3a). Such high values of the distribution coefficient cannot be explained by thermodynamics of lattice replacement reactions. It has been reported that the solubility of $BaSO_4$ increases with IS,[23,24] which would lead to a decrease in the equilibrium constant, as shown by eq 6 of the Supporting Information. However, the solubility of $RaSO_4$ would also increase with IS, which would offset the increase in $BaSO_4$ solubility. Hence, a change in the thermodynamic driving force at high salinity is an unlikely reason for enhanced radium removal.

There are several explanations for the increase in radium removal with an increase in IS. First, the activities of electrolytes decrease with an increase in IS (Table 1), which reduces supersaturation. Because nucleation of $BaSO_4$ follows the homogeneous nucleation theory with diffusion-controlled crystal growth,[25−27] a decrease in supersaturation leads to a sharp decrease in the nucleation rate[28] and a decrease in the crystal growth rate.[26] This reduction in the rate of precipitation would enhance incorporation of radium into $BaSO_4$ because it would allow more time for lattice replacement reactions during the crystal growth. In addition, the increase in IS would decrease the crystal−solution interfacial tension,[28] increase etch density,[29] and compress the electric double layer,[30] which increases the probability of the Ra^{2+} reaction with the $BaSO_4$ lattice.

A high distribution coefficient for Ra−$SrSO_4$ co-precipitation (Figure 1) is attributed to large differences in solubility products of $RaSO_4$ ($K_{sp,RaSO_4} = 10^{-10.38}$) and $SrSO_4$ ($K_{sp,SrSO_4} = 10^{-6.63}$). However, the possibility of the inclusion reaction decreases when the volumetric mismatch between the two end members (i.e., $RaSO_4$ and $SrSO_4$) is large (see Table SI-2 of the Supporting Information),[31] which would significantly depress radium incorporation into $SrSO_4$ precipitate. The mismatch phenomenon can be quantified by the Margules parameter (W), as described in Table SI-2 of the Supporting Information. The Margules-corrected distribution coefficient for Ra−$SrSO_4$ (K_d = 237) is very large compared to that for Ra−$BaSO_4$ (K_d = 1.54), which implies that $SrSO_4$ should have stronger affinity for radium. Experimental results (Figure 4a) show that radium removal in dilute solutions is always around 80%, regardless of Sr removal. Consequently, the experimental distribution coefficient for Ra−$SrSO_4$ varies from 43 to below 1 (Figure 4b) and is much lower than the theoretical value.

A significant decrease in activity coefficient ratios of ($\gamma_{Ra^{2+}}/\gamma_{M^{2+}}$) at elevated IS (see Figure SI-1 of the Supporting Information) would reduce the theoretical distribution coefficient. The theoretical distribution coefficient for Ra−$SrSO_4$ at IS = 3 M of 110 is still very large compared to Ra−$BaSO_4$ (Figure 1). Experimental results show that radium removal is greater than 75%, as long as Sr removal is greater than 8% (Figure 4a). The discrepancy of K_d and K_d' is attributed to the kinetic limit for Ra inclusion into $SrSO_4$ and underestimation of incompatibility (volumetric mismatch) of Ra−SO_4 in Sr−SO_4 lattice, which limits Ra removal at relatively

dx.doi.org/10.1021/es405168b | Environ. Sci. Technol. 2014, 48, 4596−4603

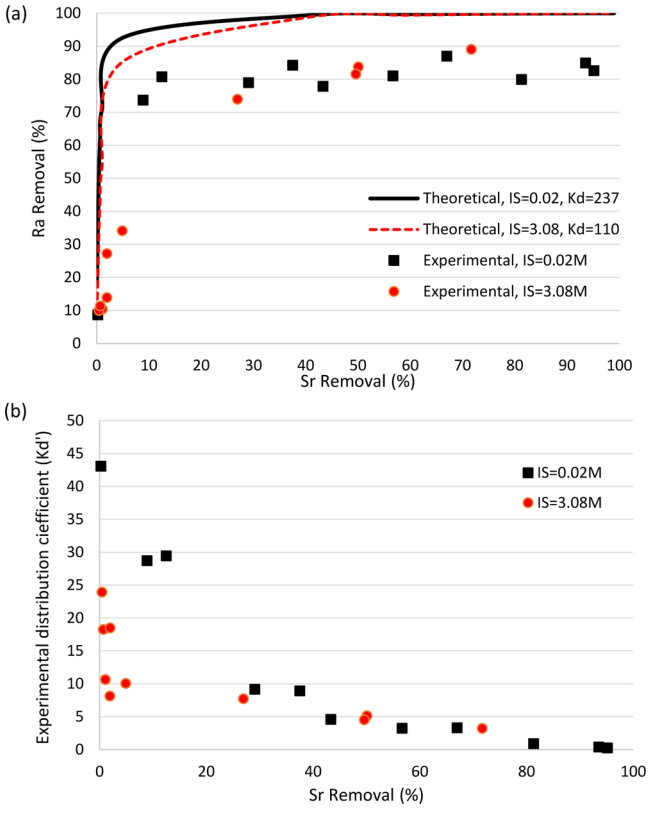

Figure 4. Radium co-precipitation with $SrSO_4$ as a function of strontium removal at different ISs adjusted with NaCl: (a) radium removal and (b) experimental distribution coefficient, at pH 7 and 5 mM Sr^{2+}initial. Sr removal is adjusted with sulfate addition (1.25−10 mM for dilute system and 5−50 mM for IS ≈ 3 M).

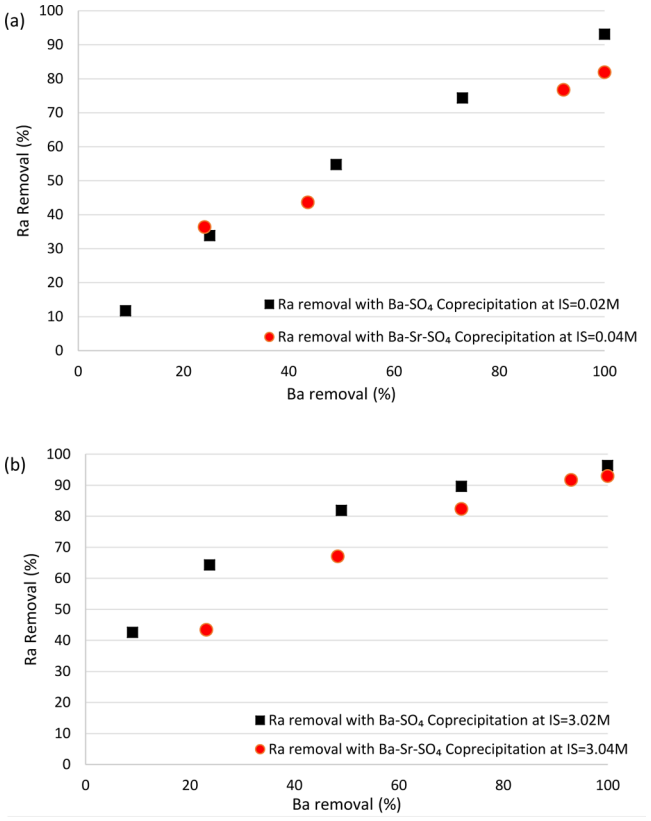

Figure 5. Radium co-precipitation with $BaSO_4$ and Ba−Sr−SO_4 systems: (a) impact of Sr addition to Ra−Ba−SO_4 in dilute solution and (b) impact of Sr addition to Ra−Ba−SO_4 in solution with elevated IS. Initial Ba and Sr concentrations were 5 mM, and Ba removal was controlled by sulfate addition (sulfate addition up to 10 mM was needed to precipitate $SrSO_4$ in the ternary system at high IS)

short reaction times (<48 h) and exacerbates the competition of Ra with other cations for the lattice replacement reaction.

Ra Removal by Co-precipitation in a Ternary System. In actual flowback and produced water from unconventional gas extraction, both barium and strontium are present at concentrations that are of the same order of magnitude.[7] Synthetic solutions used for the study of the ternary system contained 10 000 pCi/L of radium and 5 mM each of barium and strontium, and the IS was adjusted using sodium chloride. Sulfate dosage between 1.25 and 10 mM was added to control Ra−Ba−Sr−SO_4 precipitation, and radium removal was compared to barium removal as a function of IS (Table 1).

Because both $BaSO_4$ and $SrSO_4$ are good radium carriers, overall radium removal in the ternary system was expected to be enhanced by the synergy of the two co-precipitation processes. However, kinetics of $BaSO_4$ precipitation was much faster than that of $SrSO_4$ under the experimental conditions used in this study because the SI for $BaSO_4$ (from 2.6 to 4.7) was much higher than that for $SrSO_4$ (from −0.47 to 1.43). A previous study[32] showed that the kinetics of $BaSO_4$ precipitation under similar conditions was much faster than $SrSO_4$ (i.e., $BaSO_4$ precipitation was completed within 30 min, while it took several days for $SrSO_4$ to reach equilibrium). It is expected that faster $BaSO_4$ precipitation is likely to control radium removal by inclusion in the precipitate.

As shown in Figure 5, the dependence of radium removal upon barium removal in the Ra−Ba−Sr−SO_4 ternary system follows that for the Ra−Ba−SO_4 binary system. A slight decrease in Ra removal observed in the ternary system can be attributed to the presence of Sr that competes with radium for co-precipitation with $BaSO_4$.[33]

To verify that $BaSO_4$ is the main Ra carrier in the Ba−Sr−SO_4 system, precipitates created in binary and ternary systems were collected on a 0.45 μm filter membrane and added into 50 mL of 5 mM barium and strontium solution to suppress readsorption of radium on the remaining solids. Hydrochloric acid was then added to adjust pH to 0.5 and dissolve $SrSO_4$. After that, aqua regia was added to dissolve any remaining solids and radium mass balance closure above 80% was required to accept the results from these tests. Dissolution of Ra, Ba, and Sr from the solid phase at pH 0.5 is summarized in Table 2.

The results for sample A obtained using the solids precipitated in the Ra−Ba−SO_4 binary system show that very little radium was released into solution (5.4%) at pH 0.5 when $BaSO_4$ was the only radium carrier. This is expected because there was minimal (3.0%) $BaSO_4$ dissolution at pH 0.5. The test with sample B that was obtained using the solids precipitated in the Ra−Sr−SO_4 binary system showed that strontium dissolution was significant at pH 0.5 (47.0%) and that a large fraction of radium was released into the solution (73.3%) under these conditions. A higher percentage of radium released to solution compared to strontium indicates that radium is not tightly bound in the $SrSO_4$ lattice, which can be explained by the large volumetric mismatch between the two (see Table SI-2 of the Supporting Information). In sample C collected from the Ra−Ba−Sr−SO_4 ternary system, only 6.7% of radium was released to the solution after 24 h at pH 0.5,

dx.doi.org/10.1021/es405168b | Environ. Sci. Technol. 2014, 48, 4596−4603

Table 2. Radium, Barium, and Strontium Dissolution from Solids Generated in Binary and Ternary Co-precipitation Systems after 24 h at pH 0.5[a]

sample	initial concentration (mmol/L)			solids concentration (mg/L)	fraction dissolved (%)		
	Ba	Sr	SO_4		Ba	Sr	Ra
Ba–Ra–SO_4 binary	5		5	1167	3.0		5.4
Sr–Ra–SO_4 binary		5	5	918		47.0	73.3
Ba–Sr–Ra–SO_4 ternary	5	5	10	2085	3.0	51.0	6.7

[a]The initial Ra concentration in all tests was 10^4 pCi/L.

Table 3. Radium Post-precipitation Removal by Preformed Barite and Celestite[a]

adsorbent	solid concentration (g/L)	solution composition	Ra removal after 24 h (%)	Ra desorption ratio[b] (%)	Ra desorption (pCi/L)[c]
barite	0.2	DI water	84.3	36.2	3052
	0.5	DI water	84.0	19.3	1621
	1	DI water	87.2	11.6	1012
	1	5 mM Ba	32.0	24.8	794
	1	5 mM Ba; 5 mM Sr	29.5	26.4	779
	1	3 M NaCl	94.8	4.1	389
	5	5 mM Ba	66.2	15.6	1033
	10	5 mM Ba	81.9	14.1	1155
celestite	1	DI water	85.9		
	1	5 mM Sr	52.7		
	1	5 mM Ba	69.8		

[a]All samples were equilibrated for 24 h. The initial Ra concentration in all tests was 10^4 pCi/L. [b]Ra desorption ratio denotes the desorbed amount as a percentage of total Ra present in the carrier. [c]Ra desorption denotes the total activity of Ra desorbed from the carrier.

while the fractions of strontium (51.0%) and barium (3.0%) released to the solution were similar to those observed in the case of binary systems. Very low radium release from solids collected in both Ra–Ba–SO_4 and Ra–Ba–Sr–SO_4 systems confirmed that radium is mainly bound to $BaSO_4$ solids during Ra–Ba–Sr–SO_4 co-precipitation.

Co-precipitation versus Post-precipitation for Radium Removal. Co-precipitation is defined as simultaneous removal of both tracer and carrier from an aqueous solution and is due to inclusion (lattice replacement), occlusion, and adsorption reactions (Figure 2). The term post-precipitation refers to tracer removal by a previously formed carrier precipitate when only lattice replacement and adsorption are feasible removal mechanisms. Removal of Ra by preformed barite and celestite may be an important mechanism for Ra sequestration in a treatment process that uses solids recycling to enhance the precipitation kinetics in the reactor and was evaluated in this study using the experimental conditions outlined in Table 3.

The first set of experiments revealed that radium post-precipitation removal by barite did not change much even as barite concentration varied from 0.2 to 1 g/L. In addition, when radium-enriched barite was returned into a fresh radium solution [10 000 pCi/L in deionized (DI) water], radium removal was the same as for a freshly prepared barite (Table 4).

Table 4. Post-precipitation of Radium in Recycled Barite in DI Water[a]

adsorbent	solid amount (g/L)	initial Ra concentration in barite (pCi of Ra/g of barite)	solution composition (pCi/L Ra)	Ra removal (%)
barite	1	0	10000	84.30
	1	8430		87.47
	1	17177		84.87
	1	25664		85.07

[a]All samples were measured after 24 h.

Such behavior can be explained by the fact that the impurities (i.e., radium) in the $BaSO_4$ lattice are always negligible ($<2.6 \times 10^{-8}$ g of Ra/g of barite), even after 5 cycles of barite reuse, which makes fresh and reused barite identical in terms of their ability to remove radium.

To identify the extent of radium adsorption on preformed solids in comparison to inclusion, desorption studies were performed at pH 0.5 for 24 h. The desorption ratio is defined as the fraction of total radium in the solids that is released into the solution. Table 3 shows that most radium was strongly bound to the barite lattice under experimental conditions evaluated in this study. The desorption ratio decreased with increasing barite dose, suggesting that adsorption is a less significant radium removal mechanism during post-precipitation compared to inclusion.

Ra post-precipitation removal by preformed barite is strongly suppressed in the presence of Ba in solution (Table 3) because of the competition for inclusion into the barite matrix. The adverse impact of Sr in solution is not as substantial because of significant volumetric mismatch between $BaSO_4$ and $SrSO_4$. IS has a similar impact on radium incorporation into barite in the case of post-precipitation (Table 3) as it did in the case of co-precipitation (Figure 3), as demonstrated by an increase in radium removal with an increase in IS.

Radium removal by the preformed celestite was strongly depressed in the presence of competition ions (i.e., strontium or barium). This phenomenon was expected because the effective solid–solution interface area for inclusion reactions is limited in the absence of the crystal growth phase during post-precipitation uptake of radium. However, the decrease in radium removal in the presence of competing ions is less pronounced in comparison to $BaSO_4$ post-precipitation, which is expected because of the very high theoretical distribution coefficient for Ra–$SrSO_4$ and much lower solubility of $SrSO_4$.[34] Desorption of Ra–$SrSO_4$ was not evaluated because celestite is largely dissolved at pH 0.5.

dx.doi.org/10.1021/es405168b | Environ. Sci. Technol. 2014, 48, 4596–4603

Implications for Flowback/Produced Water Treatment by Sulfate Precipitation. Flowback/produced water generated from Marcellus Shale gas extraction was initially treated in municipal wastewater treatment facilities that are generally not capable of removing TDS, and high conductivities were reported in the Monongahela River basin[35] as a result of this practice. The Pennsylvania Department of Environmental Protection then issued a request in mid-2011 to exclude municipal treatment facilities from this practice and industry complied.[36] Centralized waste treatment (CWT) facilities play a major role in treatment of Marcellus Shale wastewater prior to disposal or reuse in subsequent hydrofracturing operations.[36,37] The volume of unconventional gas wastewater treated in these facilities increased from 644.4 million liters in 2008 to 1752.8 million liters in 2010.[37] Sulfate precipitation is a common practice in CWT facilities for barium, strontium, and radium removal.

On the basis of the behavior of the Ra–Ba–Sr–SO_4 ternary system at high IS documented in this study, it can be concluded that Ra inclusion in $BaSO_4$ is likely the primary mechanism for its removal in CWT facilities that employ sulfate precipitation. The experimental distribution coefficient for Ra in $BaSO_4$ ranges from 1.07 to 1.54 for dilute solution and from 1.86 to 7.49 at IS ≈ 3 M, suggesting that Ra removal in CWT facilities will be higher than Ba removal. This study also suggests that it would be beneficial to recycle barite solids in the treatment process to enhance Ra removal because recycled barite (i.e., Ra-enriched barite) showed very similar Ra removal compared to freshly prepared barite (Table 4). Once radium is incorporated into the barite lattice, it is unlikely to desorb, even at very low pH (e.g., pH 0.5).

A recent study on the impact of shale gas wastewater disposal on water quality in western Pennsylvania revealed elevated levels of radium in sediments at the point of discharge from a CWT facility.[38] Because the CWT evaluated in that study employed sulfate precipitation to achieve over 90% Ba removal, it is expected that the Ra concentration in the effluent would be about 3 orders of magnitude lower than that in the raw wastewater. A continuous low level flux of Ra into the receiving stream would lead to an increase in the Ra content of the sediments downstream of the discharge point.[38] It is also possible that some of the Ra discharge into the receiving stream would be in the form of barite solids containing co-precipitated Ra that were not captured in the CWT. A high density of barite (4.5 g/cm^3) would lead to a fairly limited transport of insoluble barite downstream of the CWT and contribute to TENORM buildup in the river sediments.

Assuming an average initial Ra and Ba concentration in flowback water treated at a CWT facility of 3000 pCi/L[38] and 5 mmol/L,[7] respectively, the estimated level of Ra activity in precipitates would range from 2571 to 18087 pCi/g of $BaSO_4$, depending upon the Ba removal and distribution coefficient (Figure 6). In comparison to TENORM limits for municipal waste landfills, which range from 5 to 50 pCi/g depending upon state regulations (http://www.tenorm.com/regs2.htm), Ra levels in the solids produced in these CWT facilities far exceed these limits. Municipal waste landfills are the main disposal alternative for this solid waste as long as they do not exceed allowed source term loading (ASTL) for TENORM on an annual basis.[39] Sustainable management of solid radioactive waste produced in these treatment facilities may require alternative management strategies. One potential approach to avoid the creation of Ra-enriched solid waste is to use carbonate precipitation for Ra removal because, unlike barite, carbonate solids generated by the treatment plant could be dissolved in mildly acidic solution and disposed by deep well injection.[40] Another alternative is to reuse the Ra-enriched barite generated at CWTs used as a weighting agent in drilling mud that is typically added to maintain the integrity of the wellbore.[41]

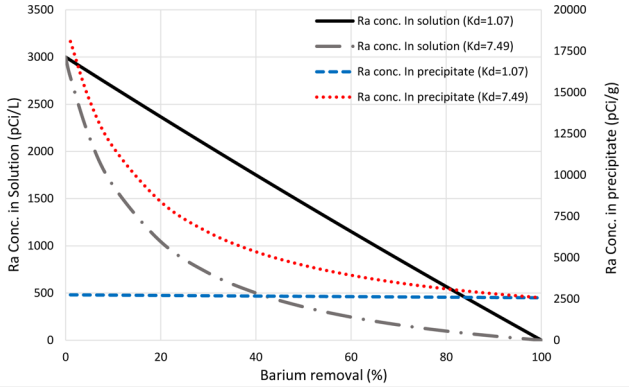

Figure 6. Theoretical radium concentrations in solution and precipitated solids resulting from sulfate addition to flowback water. Distribution coefficients for these calculations (K_d = 1.07 and 7.49) were those measured for the Ra–Ba–SO_4 binary co-precipitation system, as shown in Figure 4, at an initial Ra concentration of 3000 pCi/L and initial Ba concentration of 5 mM.

It is also important to note that municipal landfills only use γ radiation to monitor the TENORM in the incoming waste,[37] which provides only a rough estimate of Ra-226 activity because it is influenced by the composition of other radionuclides in the waste stream. A comprehensive analysis of the fate of Ra disposed in municipal solid waste landfills is needed to properly assess radiation exposure risks.[42] These risks will be associated with the emission of volatile progenies (i.e., Rn) because the results of this study suggest that Ra will not leach out in a relatively mildly acidic environment of municipal solid waste landfills[43] once it is sequestered in barite solids.

■ ASSOCIATED CONTENT

Ⓢ Supporting Information

Additional details on the derivation of the distribution coefficient and activity coefficient ratios for divalent cations of interest in this study. This material is available free of charge via the Internet at http://pubs.acs.org.

■ AUTHOR INFORMATION

Corresponding Author

*Telephone: +1-412-624-9870. Fax: +1-412-624-0135. E-mail: vidic@pitt.edu.

Notes

The authors declare no competing financial interest.

■ ACKNOWLEDGMENTS

As part of the National Energy Technology Laboratory's Regional University Alliance (NETL–RUA), a collaborative initiative of the NETL, this study was performed under Task Release TR 131, Project Activity 4.605.920.009.812.

■ REFERENCES

(1) Rowan, E.; Engle, M.; Kirby, C.; Kraemer, T. *Radium Content of Oil-and Gas-Field Produced Waters in the Northern Appalachian Basin*

(USA)—Summary and Discussion of Data; U.S. Geological Survey Scientific Investigations Report 2011-5135; U.S. Geological Survey: Reston, VA, 2011.
(2) Vidic, R. D.; Brantley, S. L.; Vandenbossche, J. M.; Yoxtheimer, D.; Abad, J. D. Impact of shale gas development on regional water quality. *Science* **2013**, *340*, 6134.
(3) Grundl, T.; Cape, M. Geochemical factors controlling radium activity in a sandstone aquifer. *Ground Water* **2006**, *44* (4), 518−527.
(4) U.S. Nuclear Regulatory Commission. *Standards for Protection against Radiation—Appendix B—Radionuclide Table-Radium-226*; U.S. Nuclear Regulatory Commission: Rockville, MD, 2013; 10 CFR, 20.
(5) Gregory, K. B.; Vidic, R. D.; Dzombak, D. A. Water management challenges associated with the production of shale gas by hydraulic fracturing. *Elements* **2011**, *7* (3), 181−186.
(6) Gordon, L.; Rowley, K. Coprecipitation of radium with barium sulfate. *Anal. Chem.* **1957**, *29* (1), 34−37.
(7) Barbot, E.; Vidic, N. S.; Gregory, K. B.; Vidic, R. D. Spatial and temporal correlation of water quality parameters of produced waters from devonian-age shale following hydraulic fracturing. *Environ. Sci. Technol.* **2013**, *47* (6), 2562−2569.
(8) Fakhru'l-Razi, A.; Pendashteh, A.; Abdullah, L. C.; Biak, D. R. A.; Madaeni, S. S.; Abidin, Z. Z. Review of technologies for oil and gas produced water treatment. *J. Hazard. Mater.* **2009**, *170* (2), 530−551.
(9) Langmuir, D.; Riese, A. C. The thermodynamic properties of radium. *Geochim. Cosmochim. Acta* **1985**, *49* (7), 1593−1601.
(10) Li, M. Removal of divalent cations from marcellus shale flowback water through chemical precipitation. Master's Dissertation, University of Pittsburgh, Pittsburgh, PA, 2011.
(11) Prieto, M. Thermodynamics of solid solution−aqueous solution systems. *Rev. Mineral. Geochem.* **2009**, *70* (1), 47−85.
(12) Doerner, H. A.; Hoskins, W. M. Co-precipitation of radium and barium sulfates. *J. Am. Chem. Soc.* **1925**, *47* (3), 662−675.
(13) Risthaus, P.; Bosbach, D.; Becker, U.; Putnis, A. Barite scale formation and dissolution at high ionic strength studied with atomic force microscopy. *Colloids Surf., A* **2001**, *191* (3), 201−214.
(14) Gordon, L.; Reimer, C. C.; Burtt, B. P. Distribution of strontium within barium sulfate precipitated from homogeneous solution. *Anal. Chem.* **1954**, *26* (5), 842−846.
(15) Harvey, D. *Modern Analytical Chemistry*; McGraw-Hill: New York, 2000.
(16) Nichols, M. L.; Smith, E. C. Coprecipitation with barium sulfate. *J. Phys. Chem.* **1941**, *45* (3), 411−421.
(17) Fischer, R. B.; Rhinehammer, R. B. Rapid precipitation of barium sulfate. *Anal. Chem.* **1953**, *25* (10), 1544−1548.
(18) Schneider, F.; Rieman, W., III The mechanism of coprecipitation of anions by barium sulfate. *J. Am. Chem. Soc.* **1937**, *59* (2), 354−357.
(19) Blackburn, R.; Al-Masri, M. S. Determination of radium-226 in aqueous samples using liquid scintillation counting. *Analyst* **1992**, *117* (12), 1949−1951.
(20) *Applications of Liquid Scintillation Counting*; Horrocks, D., Ed.; Academic Press: Waltham, MA, 1974.
(21) Johnston, A.; Martin, P. Rapid analysis of ^{226}Ra in waters by gamma-ray spectrometry. *Appl. Radiat. Isot.* **1997**, *48* (5), 631−639.
(22) Rosenberg, Y. O.; Metz, V.; Ganor, J. Co-precipitation of radium in high ionic strength systems: 1. Thermodynamic properties of the Na−Ra−Cl−SO_4−H_2O system—Estimating Pitzer parameters for $RaCl_2$. *Geochim. Cosmochim. Acta* **2011**, *75* (19), 5389−5402.
(23) Bokern, D. G.; Hunter, K. A.; McGrath, K. M. Charged barite−aqueous solution interface: Surface potential and atomically resolved visualization. *Langmuir* **2003**, *19* (24), 10019−10027.
(24) Meissner, H. P.; Tester, J. W. Activity coefficients of strong electrolytes in aqueous solutions. *Ind. Eng. Chem. Process Des. Dev.* **1972**, *11* (1), 128−133.
(25) Fernandez-Diaz, L.; Putnis, A.; Cumberbatch, J. Barite nucleation kinetics and the effect of additives. *Eur. J. Mineral.* **1990**, *2* (4), 495−501.
(26) Nielsen, A. E.; Toft, J. M. Electrolyte crystal growth kinetics. *J. Cryst. Growth* **1984**, *67* (2), 278−288.
(27) He, S.; Oddo, J. E.; Tomson, M. B. The nucleation kinetics of barium sulfate in NaCl solutions up to 6 *m* and 90 °C. *J. Colloid Interface Sci.* **1995**, *174* (2), 319−326.
(28) Anderson, G. M., Crerar, D. A. *Thermodynamics of Geochemistry: The Equilibrium Model*; Oxford University Press: New York, 1993; Vol. *588*.
(29) Risthaus, P.; Bosbach, D.; Becker, U.; Putnis, A. Barite scale formation and dissolution at high ionic strength studied with atomic force microscopy. *Colloids Surf., A* **2001**, *191* (3), 201−214.
(30) Hang, J. Z.; Zhang, Y. F.; Shi, L. Y.; Feng, X. Electrokinetic properties of barite nanoparticles suspensions in different electrolyte media. *J. Mater. Sci.* **2007**, *42* (23), 9611−9616.
(31) Zhu, C. Coprecipitation in the barite isostructural family: 1. Binary mixing properties. *Geochim. Cosmochim. Acta* **2004**, *68* (16), 3327−3337.
(32) He, C.; Li, M.; Liu, W.; Barbot, E.; Vidic, R. D. Kinetics and equilibrium of barium and strontium sulfate formation in Marcellus Shale flowback water. *J. Environ. Eng.* **2014**, DOI: 10.1061/(ASCE) EE.1943-7870.0000807.
(33) Ceccarello, S.; Black, S.; Read, D.; Hodson, M. E. Industrial radioactive barite scale: Suppression of radium uptake by introduction of competing ions. *Miner. Eng.* **2004**, *17* (2), 323−330.
(34) Brower, E. Synthesis of barite, celestite and barium−strontium sulfate solid solution crystals. *Geochim. Cosmochim. Acta* **1973**, *37* (1), 155−158.
(35) Kargbo, D. M.; Wilhelm, R. G.; Campbell, D. J. Natural gas plays in the Marcellus Shale: Challenges and potential opportunities. *Environ. Sci. Technol.* **2010**, *44* (15), 5679−5684.
(36) Maloney, K. O.; Yoxtheimer, D. A. Production and disposal of waste materials from gas and oil extraction from the Marcellus Shale play in Pennsylvania. *Environ. Pract.* **2012**, *14* (4), 278−287.
(37) Lutz, B. D.; Lewis, A. N.; Doyle, M. W. Generation, transport, and disposal of wastewater associated with Marcellus Shale gas development. *Water Resour. Res.* **2013**, *49* (2), 647−656.
(38) Warner, N. R.; Christie, C. A.; Jackson, R. B.; Vengosh, A. Impacts of shale gas wastewater disposal on water quality in western Pennsylvania. *Environ. Sci. Technol.* **2013**, *47* (20), 11849−11857.
(39) Pennsylvania Department of Environmental Protection. *Final Guidance Document on Radioactivity Monitoring at Solid Waste Processing and Disposal Facilities*; Pennsylvania Department of Environmental Protection: Harrisburg, PA, 2004; http://www.elibrary.dep.state.pa.us/dsweb/Get/Document-48337/250-3100-001.pdf.
(40) Research Partnership to Secure Energy for America (RPSEA). *Produced Water Treatment for Water Recovery and Salt Production*; RPSEA: Sugar Land, TX, 2012; 08122-36-Final Report.
(41) Oakley, D.; Cullum, D. *Advanced Technology Makes New Use of Age-Old Drilling Fluid Agent*; Drilling Contractor: Houston, TX, May/June 2007; http://www.drillingcontractor.org/dcpi/dc-mayjune07/DC_May07_MISWACO.pdf.
(42) Smith, K. P.; Arnish, J. J.; Williams, G. P.; Blunt, D. L. Assessment of the disposal of radioactive petroleum industry waste in nonhazardous landfills using risk-based modeling. *Environ. Sci. Technol.* **2003**, *37* (10), 2060−2066.
(43) United States Environmental Protection Agency (U.S. EPA). *Method 1311. Toxicity Characteristic Leaching Procedure*; U.S. EPA: Washington, D.C., 1992; http://www.epa.gov/osw/hazard/testmethods/sw846/pdfs/1311.pdf.